Int J Clin Exp Pathol 2016;9(10):10080-10092
www.ijcep.com /ISSN:1936-2625/IJCEP0036941

Original Article

Correlation between morphological and molecular changes in a rat model of partial urinary bladder obstruction and the potential effect of kaempferol

Eman M Mohamed[1], Samia A Abd El-Baset[1], Rehab S Abdul-Maksoud[2], Asmaa AA Kattaia[1]

[1]Department of Histology and Cell Biology, Faculty of Medicine, Zagazig University, Egypt; [2]Department of Biochemistry, Faculty of Medicine, Zagazig University, Egypt

Received July 30, 2016; Accepted September 20, 2016; Epub October 1, 2016; Published October 15, 2016

Abstract: Recent investigations provide evidence for the role of oxidative injury in the progression of bladder dysfunction after partial bladder outlet obstruction (PBOO). It is of interest to study the correlation between the morphological and molecular changes induced by bladder obstruction and to investigate the efficacy of kaempferol. Twenty-four rats were randomly divided into: group 1 sham-operated control rats; group 2 sham-operated rats received oral kaempferol (100 mg/kg/day); group 3 PBOO rats; group 4 PBOO rats received oral kampferol at the same dose. Four weeks after surgery, urinary bladders were processed for histopathological examinations by light and electron microscopes, real-time RT-PCR analysis [smooth muscle myosin (SMM), non-muscle myosin (NMM) and isoforms of caldesmon (h-CaD and l-CaD) mRNA] and biochemical assays [catalase (CAT), superoxide dismutase (SOD) and nitric oxide (NO) levels]. Mast cell count and immunohistochemical localization of Ki-67 and muscle actin were carried out. PBOO induced deleterious histopathological changes, increase in Ki-67 and muscle actin immune expressions, down regulation of SMM and h-CaD mRNA and up regulation of NMM and l-CaD mRNA and enhancement of tissue oxidative stress markers. Kaempferol effectively reversed these alterations through its antioxidant, anti-proliferative and anti-inflammatory capacity. The clinical application of kaempferol could represent a novel approach for counteracting bladder injury due to PBOO.

Keywords: Morphological, molecular changes, bladder obstruction, rat, kaempferol

Introduction

Bladder outlet obstruction (BOO) is a prevalent clinical issue that happens in numerous ailments, such as benign prostatic hyperplasia (BPH) in male [1] and pelvic organ prolapse in female [2]. Patients with BOO go through an initial stage of adaptation, followed by a compensation stage with stable bladder structure and function before progressing to decompensation [3]. Urinary tract complications include post void residual urine retention, bladder diverticula, hydronephrosis, bladder calculi, and renal insufficiency [4]. In chronic cases, renal failure may occur [5].

Smooth muscle myosin (SMM) is composed of a pair of myosin heavy chains (MHCs) and two pairs of intertwined myosin light chains. SMM isoforms, predominantly found in the urinary bladder, demonstrate a faster more phasic contractile nature [6]. Non-muscle myosin (NMM) II is a member of the myosin class II family. The expression of NMM in bladder smooth muscles ranges between 0 and 10% of total myosin and may contribute to tonic force maintenance [7].

Caldesmon (CaD) is an actin-associated protein, expressed as two isoforms, l-CaD and h-CaD. l-CaD is found in non-muscle cells whereas h-CaD is bound to thin filaments in smooth muscle cells. h-CaD regulates smooth muscle contraction, via the phosphorylation of myosin light chain [8]. In PBOO, the overexpression of l-CaD could be useful in estimating the degree of detrusor contractile dysfunction [9].

Flavonoids are polyphenol compounds naturally exist in many plants and botanical products commonly used in traditional medicine [10].

Flavonoids have become popular in terms of health protection because of their anti-ischemic, vaso-relaxant and anti-oxidant activities [11]. Among them, Kaempferol (3,5,7-trihydroxy-2-(4-hydroxyphenyl)-4H-1-benzopyran-4-flavone) is widely present in broccoli, chives, tea, grapes, tomatoes and strawberries [12]. The antioxidant activity of several flavonoids was evaluated and kaempferol is considered as one of the strongest scavengers for the fenton-generated hydroxyl radical [13]. Kaempferol also has anti-carcinogenic, cardio-protective, anti-aging and anti-postmenopausal bone loss properties [14-16].

Many patients undergo obstruction relief procedures such as prostatectomy but many of them still report persistent storage symptoms [17]. So, it is vital to look for suitable and successful management.

Accordingly, the aim of our study is to correlate the morphological and molecular changes induced by bladder obstruction and to investigate efficacy of kaempferol in improving these changes in a rat model of PBOO.

Material and methods

Chemicals

Kaempferol (yellow powder; CAS No. 520-18-3; purity of ≥ 97%) was purchased from Sigma-Aldrich (St. Louis, MO, USA) and stored in a dark container at room temperature.

Experimental animals

Twenty-four adult male albino rats (200-250 g weight; 7-9 week age) were obtained from the Breeding Animal House of the Faculty of Medicine, Zagazig University, Egypt. The animals were housed in plastic cages with stainless steel wire-bar lid and maintained under standard laboratory conditions at 23 ± 1°C, relative humidity 55 ± 5% and photoperiod of 12 h-dark and light. They were fed with commercial pellet diet and allowed ad libitum access to food and drinking water. Animals were acclimatized to the laboratory conditions for 7 days prior to the experiment. All studies were performed in accordance with institutional guidelines for the care and use of experimental animals and approved by the Ethical Committee of Zagazig University (Egypt).

Experimental protocol

Rats were randomly divided into 4 groups (6 rats each) and maintained for 4 weeks. Group 1 served as sham-operated control rats. Group 2 was sham-operated and supplemented with kaempferol (100 mg/kg b. w./day; dissolved in 5% dimethylsulfoxide [DMSO]; by oral gavage) [18-20]. Group 3 was subjected to partial bladder outlet obstruction (PBOO) [21]. Group 4 consisted of PBOO rats that received kampferol at the same previous dose and route. Kampferol administration started after PBOO induction following a previously published method [22].

Operative procedures

Animals were anaesthetized with intramuscular injection of ketamine (15 mg/kg) and xylazine (5 mg/kg) [23]. The bladder base and proximal urethra were exposed through a lower midline incision. A 4-0 nylon thread was tied loosely around the urethra in the presence of an intraluminal indwelling polyethylene tube (1 mm in diameter). The abdomen wall was closed after the polyethylene tube was removed leaving the urethra partially obstructed.

The sham-operated rats underwent the same procedures except that the thread placed around the proximal urethra and the polyethylene tube was not tied. Ampicillin (50 mg/kg/day) was administered via drinking water for 3 days to prevent postoperative infection [24].

At the end of the experimental period, rats were sacrificed by intra-peritoneal administration of pentobarbital (40 mg/kg). The bladder of each animal was dissected out carefully and blotted dry. A part of the bladder was used for biochemical assays and the other for histological assessment. For biochemical analysis, tissues were frozen immediately in liquid nitrogen and stored at -80°C until the preparation of tissue homogenates.

Histopathological study

Haematoxylin and eosin (H&E) stain: Specimens for light microscopy were fixed in 10% saline formalin and processed to prepare 5-µm-thick paraffin sections for H&E stain [25].

Ultrastructural study: Specimens for electron microscopy were immediately fixed in 2.5%

phosphate-buffered glutaraldehyde (pH 7.4), post fixed in 1% osmium tetroxide in the same buffer at 4°C, dehydrated and embedded in epoxy resin. Ultrathin sections were obtained (Leica ultra-cut UCT), stained with uranyl acetate and lead citrate [26], examined and photographed (JEOL JEM 1010 transmission electron microscope; Jeol Ltd, Tokyo, Japan) in the Regional Center of Mycology and Biotechnology (RCMB), Al-Azhar University, Egypt.

Toluidine blue stain: Semi-thin sections were also obtained (Leica ultra-cut UCT), stained with toluidine blue and examined by light microscope.

Immunohistochemical study: Immunohistochemical staining for localization of Ki-67 and muscle actin was carried out by means of the avidin biotin complex (ABC) method (Dako ARK™, Peroxidase, Code No. K3954, Dako, Glostrup, Denmark) following the manufacturer's instructions.

Paraffin sections (4 μm) were dewaxed, hydrated and microwaved in citrate buffer, pH 6, for antigen retrieval. Endogenous peroxidase was eliminated by incubation in 10% H_2O_2 in phosphate-buffered saline (PBS), pH 7.4. Nonspecific binding was blocked in a normal mouse serum at room temperature. Then, the sections were incubated with the specific primary antibody overnight (4°C): anti Ki-67 antibody (rabbit polyclonal antibody; No. ab15580; dilution 1 μg/ml; Abcam, Cambridge, UK) and anti- muscle actin antibody (rabbit monoclonal antibody; No. ab156302; dilution 1/250; Abcam, Cambridge, UK). The sections were incubated with biotinylated secondary antibodies followed by labeled horseradish peroxidase. 3, 3'-diaminobenzidine (DAB) was used as chromogen that resulted in a brown-colored precipitate at the antigen site. Sections were counterstained with haematoxylin. Negative control sections were incubated with PBS instead of the primary antibody. Stained slides were analyzed by light microscopy [27].

Real-time reverse transcriptase polymerase chain reaction (RT-PCR)

Total RNA was extracted from the frozen bladder tissues using TRIzol reagent (Invitrogen; Carlsbad, CA, USA) according to the manufacturer's protocol. The resulting RNA was quantitated by spectrophotometry at 260/280 nm. RNA was reverse transcribed into complementary DNA (cDNA) using a Quanti Tect Reverse Transcription Kit (Qiagen). SYBR Green PCR kit (Roche Diagnostics) and cDNA synthesized from 1 μg total RNA in a 20 μL reaction volume were subjected to PCR according to the manufacturer's instructions. In all reactions, GAPDH was used as a housekeeping gene for standardization. For smooth muscle myosin (SMM), non-muscle myosin (NMM) and caldesmon isoforms (h-CaD and l-CaD), the following primer pairs (Operon, Huntsville, AL) were used: SMM heavy chain (Forward 5'-TTTGCCATTGAGGCCTTAGG-3'; Reverse 5'-TTTGCCATTGAGGCCTTAGG-3'), NMM heavy chain (Forward 5'-TGAGAAGCCGCCACACATC-3'; Reverse 5'-CACCCGTGCAAAGAATCGA-3'), h-CaD (Forward 5'-CAGAAGGGAAGTCGGTAAATGAAA-3'; Reverse 5'-TCTTCTTTGGCCTCTTTGTCCTT-3'), l-CaD (Forward 5'-CAAATCCGAGCAGAAGAATGACTG-3'; Reverse 5'-TCTTCTTTGGCCTCTTTGTCCTT-3'], GAPDH (Forward 5'-CCTCGTCTCATAGACAAGATGGT-3'; Reverse 5'-GGGTAGAGTCATACTGGAACATG-3'). All samples were run in duplicates and PCR reactions were performed according to the following protocol: denaturation at 95°C for 10 min followed by 40 cycles of 95°C for 15 s, then 60°C for 60 s. PCR products were electrophoresed on 2% agarose gel stained with ethidium bromide and visualized by UV detector (BioRad Laboratories Inc., Hercules, CA). The final PCR product for each sample was quantified using a computing densitometer (Gel Doc EQ; Biorad Laboratories, Hercules, CA) and software (Quantity One). The relative expression of each gene was calculated as the ratio of the respective gene amplified to that of the housekeeping gene. Altered mRNA levels in experimental groups were expressed as fold changes based on $2^{-\Delta\Delta CT}$ analysis.

Biochemical analysis of tissue antioxidant enzymes

Bladder homogenates preparation: Tissues were homogenized in ice-cold phosphate buffered saline (pH 7.4). The homogenates were centrifuged (8000× g, 30 min, 4°C) to obtain cell-free supernatant. Commercially available kits (Bio Diagnostic Company, Dokki, Giza, Egypt) were used for biochemical analysis.

Catalase (CAT): CAT activity was measured by the decrease in the concentration of hydrogen

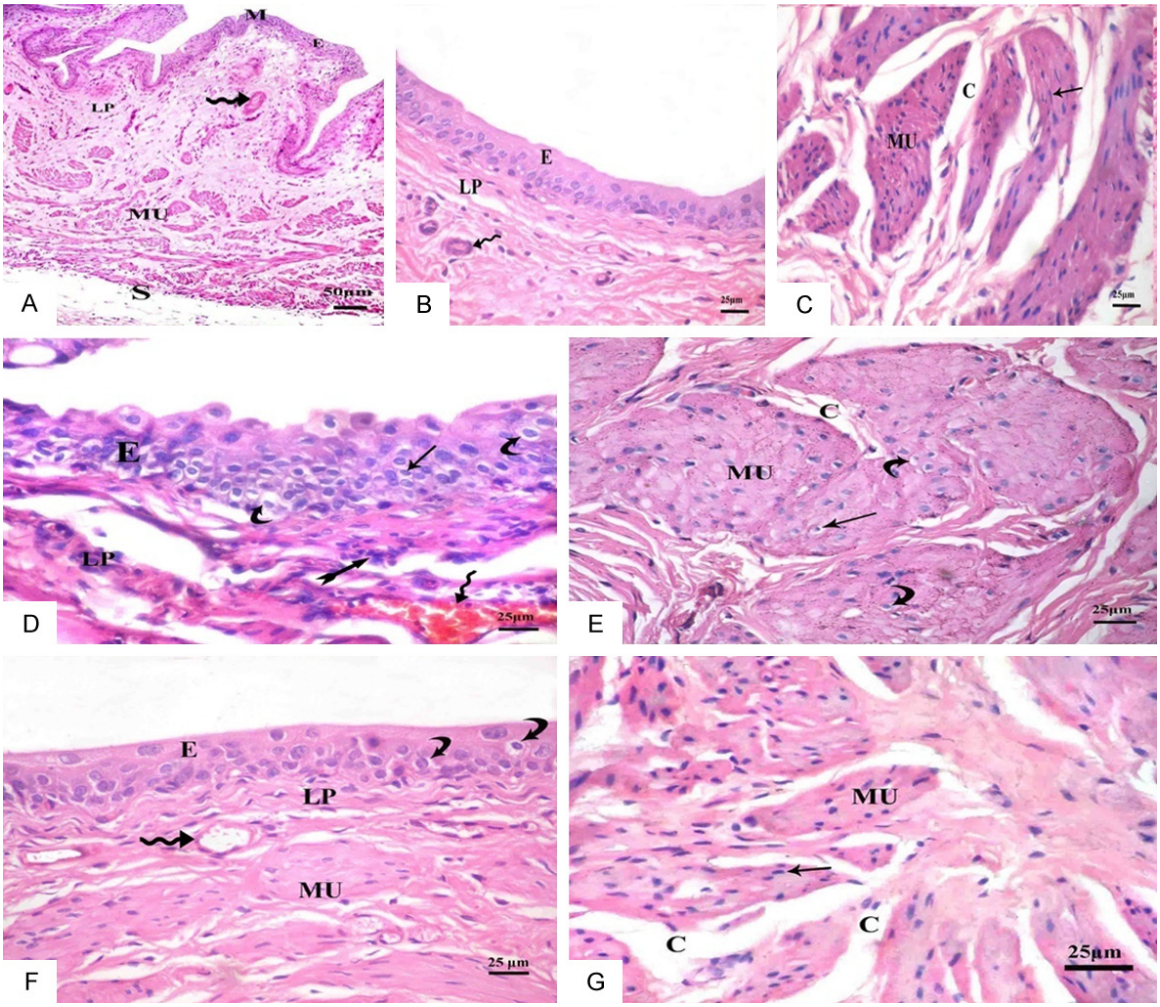

Figure 1. H&E-stained sections in urinary bladder of albino rats of the study groups. A-C: Group 1, mucosa (M), transitional epithelium (E), lamina propria (LP) blood capillaries (wavy arrow), Musculosa (MU), Serosa (S). Nuclei of smooth muscle fibers (arrow), connective tissue (C). D and E: Group 3, transitional epithelium (E), dark stained nuclei (arrow), cytoplasmic vacuolations (curved arrow), lamina propria (LP), cellular infiltration (bifid arrow), congested blood vessel (wavy arrow), thick musculosa (MU), interstitial connective tissue (C). F and G: Group 4, transitional epithelium (E), vacuolated cells (curved arrow), lamina propria (LP), blood capillaries (wavy arrow), nearly normal muscle layer (MU), nuclei (arrow), connective tissue (C).

peroxide after incubation with various volumes of the homogenates, as described earlier [28]. Results were expressed as units per milligram of protein.

Superoxide dismutase (SOD): The SOD measurement was based on the principle that xanthine reacts with xanthine oxidase to form superoxide radicals, that form a red formazon dye when react with INT (2-(4-iodophenyl)-3-(4-nitrophenol)-5-phenyltetrazolium chloride). The SOD activity is assayed by the degree of inhibition of this reaction [29]. Results were expressed as units per milligram of protein.

Nitric oxide assay: Combined nitrate/nitrite (NOx) measurement was used to determine total NO concentration using a nitrate/nitrite fluorometric assay kits. Nitrate is converted to nitrite by nitrate reductase. Nitrite reacts with the fluorescent probe DAN (2, 3 diaminonaphthalene). The fluorescent intensity is proportional to the total nitric oxide production. Results were expressed as mmol/mg protein [30].

Morphometric study

The Leica QWin 500 image analyzer computer system (Leica Ltd, Cambridge, UK) was used.

The data analyzed by Leica QWin 500 software with the aid of a digital camera connected to an optical microscope (Olympus). The thickness of epithelium (μm) and muscle coat (mm) was measured in H&E stained sections. Positive cells in anti-Ki 67 immune stained sections and mast cells in toluidine blue-stained sections were counted. The area percentage of positive immune reactivity in anti-muscle actin immune-stained sections was also measured.

All measurements were evaluated on images captured at a final magnification (400×) except for mast cell count (1000×). Using the interactive measure menu, 5 non-overlapping fields were analysed per each slide for each animal. The measurements were performed by an investigator who is blinded to the source of the samples and the results.

Statistical analysis

SPSS statistical software version 20 for Windows was used to evaluate the data. Values were expressed as means ± standard error of means (SEM). Data were statistically analyzed by using ANOVA test followed by post hoc multiple comparisons. The probability values (*P*) less than 0.05 were considered significant and highly significant when the *P* values were less than 0.001 [31].

Results

Histopathological results

The light and electron microscopic examinations of groups 1 and 2 showed similar results. Only morphological results of the control group 1 were presented.

H&E stain results: Light microscope examination of group 1 revealed normal structure of the urinary bladder; mucosa, musculosa and serosa (**Figure 1A**). The folded mucosa composed of transitional epithelium and underlying lamina propria (**Figure 1B**). The musculosa is formed of smooth muscle fibers with acidophilic cytoplasm and elongated nuclei arranged in different directions and separated by interstitial connective tissue (**Figure 1C**).

The transitional epithelium of group 3 appeared thick with dark stained nuclei and cytoplasmic vacuolations around the nuclei of many cells. The lamina propria contained cellular infiltration and congested blood vessels (**Figure 1D**). The musculosa was formed of thickened smooth muscle fibers with acidophilic cytoplasm and some shrunken nuclei (**Figure 1E**).

Examination of group 4 showed nearly normal structure of the bladder mucosa and musculosa away from few vacuolated urothelial cells (**Figure 1F** and **1G**).

Ultrastructural changes: Electron microscope examination of group 1 revealed that the cells of superficial layers of transitional epithelium had euchromatic nuclei, angulated luminal border and lenticular vesicles. Junctional complexes and extensive membrane interdigitations appeared between adjacent cells (**Figure 2A** and **2B**). The basal epithelial cells had euchromatic nuclei and cellular interdigitations. They rested on regular basement membrane with underlying connective tissue (**Figure 2C**). Smooth muscle fibers of the musculosa were separated by narrow intercellular spaces with few collagen fibrils in between. Their cytoplasm contained dense bodies and dense plaques under the sarcolemma (**Figure 2D**).

The ultrathin sections of group 3 showed widened intercellular spaces and disrupted junctional complexes between the cells of the superficial and middle layers of the urothelium. The urothelial cells appeared with irregular heterochromatic nuclei and vacuolations (**Figure 2E** and **2F**). Neutrophils were detected in between the urothelial cells; they had lobulated nuclei and lysosomes rich cytoplasm (**Figure 2G**). Some mast cells were seen in between the cells of the transitional epithelium, they had heterochromatic nuclei and different sized electron dense granules (**Figure 2H**). Lamina propria showed increased collagen fibrils and mast cells compared with group 1 (**Figure 2I**). Myocytes revealed indistinct dense bodies. The intercellular spaces were widened and filled with increased collagen fibrils (**Figure 2J**).

Examination of ultrathin sections of group 4 revealed more or less normal transitional epithelial cells with euchromatic nuclei. The superficial cells had few cytoplasmic vacuolations and restored cellular interdigitations and junctions. The basal cell layer rested on regular basement membrane and the cells were adherent to each other (**Figure 2K** and **2L**). Myocytes appeared with normal dense bodies, narrow

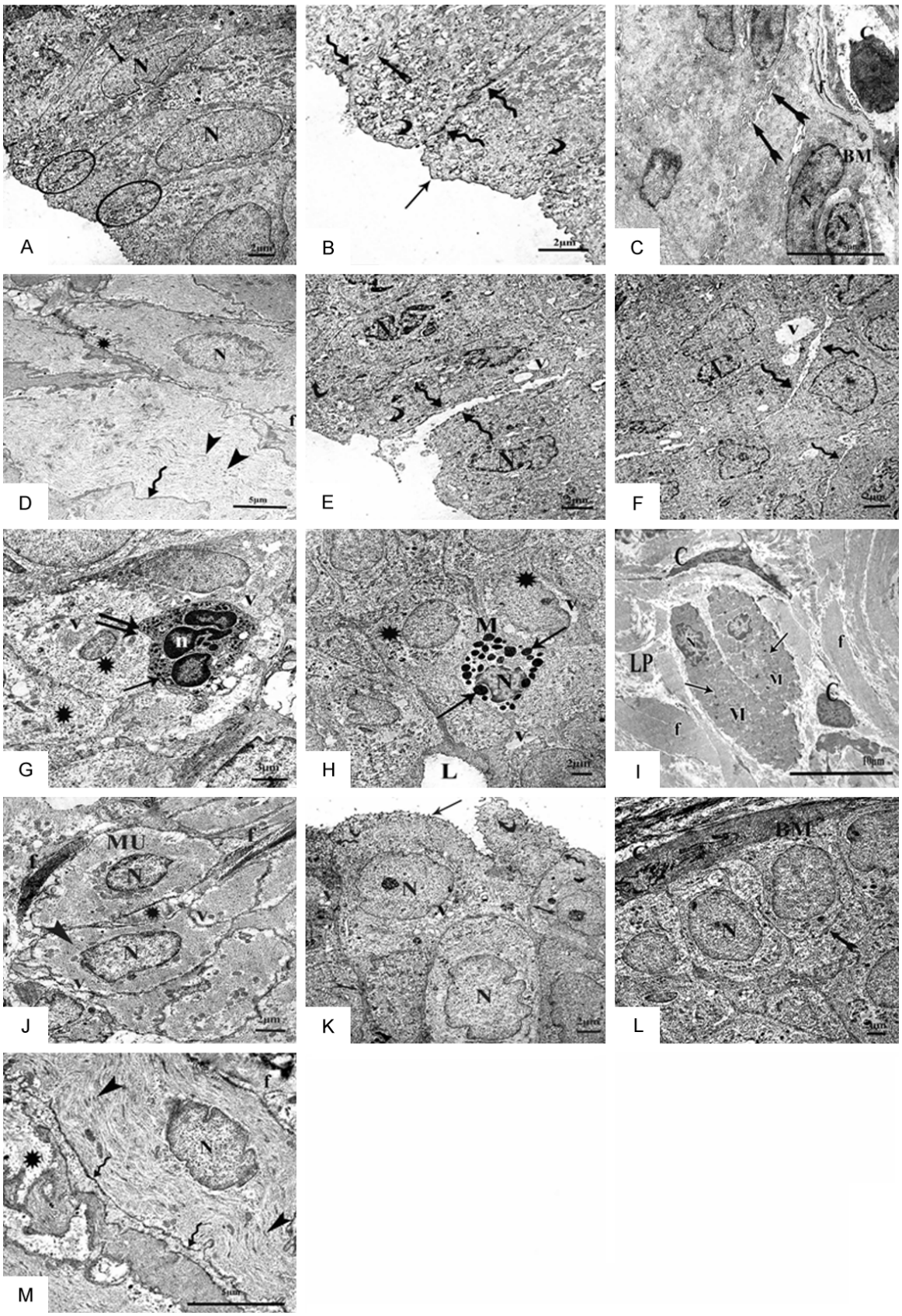

Figure 2. An electron micrograph of sections in the urinary bladder of adult male rats of all study groups. A-D: Group 1. A: Superficial layers of transitional epithelium, euchromatic nuclei (N), cellular interdigitations (bifid arrow), cel-

lular junction (ovoid shape). B: Higher magnification, angulated luminal border (arrow), lenticular vesicles (curved arrow), membrane interdigitations (bifid arrow), junction (wavy arrow). C: Basal layers of transitional epithelium, regular basement membrane (BM), collagen fibers (F), connective tissue cells (C), cellular interdigitations (bifid arrow), euchromatic nuclei (N). D: Smooth muscle fibers with minimal intercellular spaces (*), collagen fibrils (F), dense bodies (arrow head), dense plaques (wavy arrow). E-J: Group 3. E&F: Superficial and middle layers of transitional epithelium, lenticular vesicles (curved arrow), vacuolations (V) irregular heterochromatic nuclei (N), disrupted junctional complexes (wavy arrow). G: Neutrophils (double arrow), lobulated nucleus (N), lysosomes (arrow), urothelial cells (*), vacuolations (V). H: Mast cells (M) with granules (arrow), heterochromatic nucleus(N), urothelial cells (*), vacuolations (V), lumen (L). I: Lamina propria (LP), connective tissue cells (C), collagen fibrils (F), mast cells (M), granules (arrow), heterochromatic nucleus (N). (J) Smooth muscle cells (MU), indistinct dense bodies (arrow head), nucleus (N), vacuolations (V), wide intercellular spaces (*), increased collagen fibrils (F). K-M: Group 4. K&L: Superficial and basal layers of urothelium with angulated luminal border (arrow), lenticular vesicles (curved arrow), cellular interdigitations (bifid arrow), intercellular junctions (wavy arrow), euchromatic nuclei (N), vacuolations (V), regular basement membrane (BM), connective tissue cell (C). M: Myocytes (MU), nuclei (N), dense bodies (arrow head), dense plaques (wavy arrow), intercellular spaces (*), collagen fibrils (F).

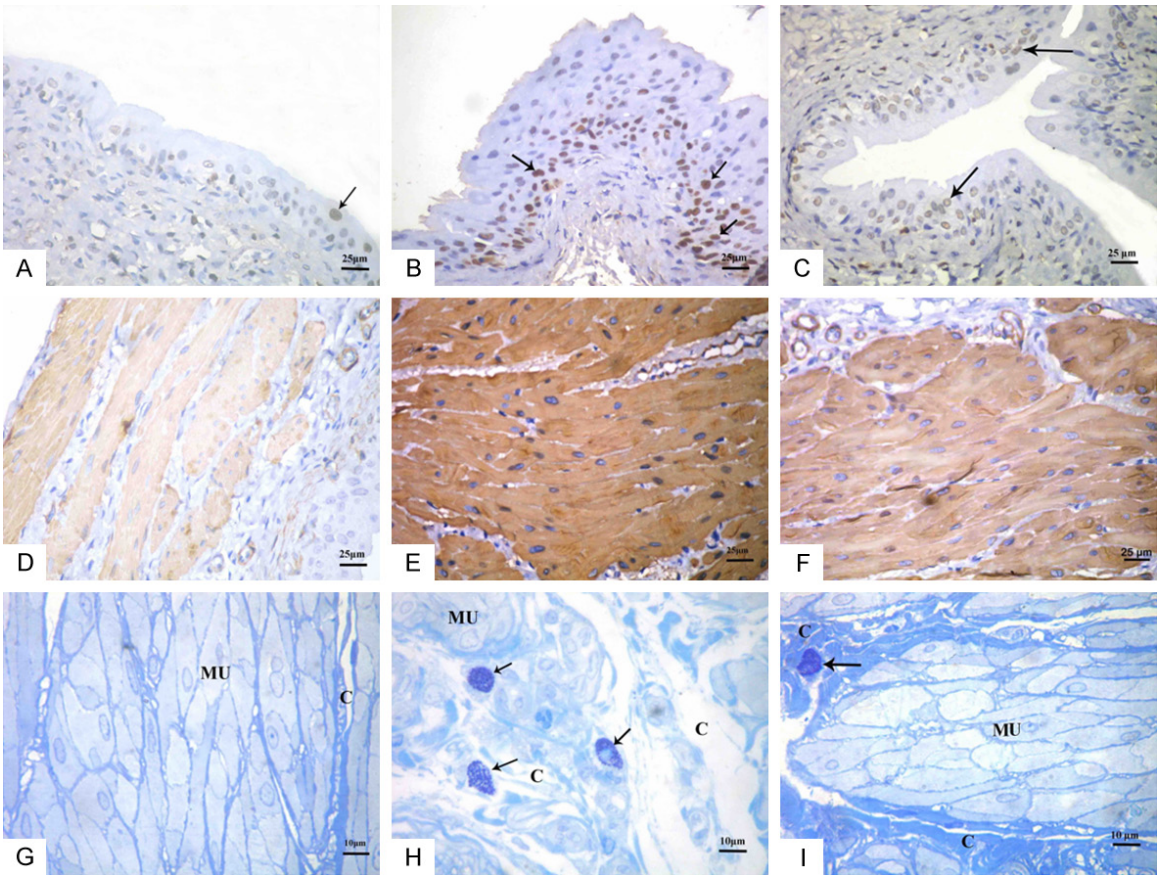

Figure 3. Sections in the urinary bladder of albino rats of study groupS. A, D, G: Group 1. B, E, H: Group 3. C, F, I: Group 4. A-C: Nuclear immune reaction for ki 67, positive reactions (arrow). D-F: Cytoplasmic immune reaction for muscle Actin. G-I: Toluidine blue stained semi-thin sections, mast cells (arrow), connective tissue (C), muscle fibers (MU).

intercellular spaces and collagen fibers (**Figure 2M**).

Toluidine blue stain results: Examination of semi-thin sections stained with Toluidine blue revealed scanty mast cells in group 1 (**Figure 3G**). Group 3 showed increased number of mast cells in the connective tissue between the muscle fibers of musculosa compared with group 1 (**Figure 3H**). The number of mast cells was about normal in group 4 (**Figure 3I**).

Immunohistochemical results: Immunohistochemically stained sections for Ki 67 of group 1

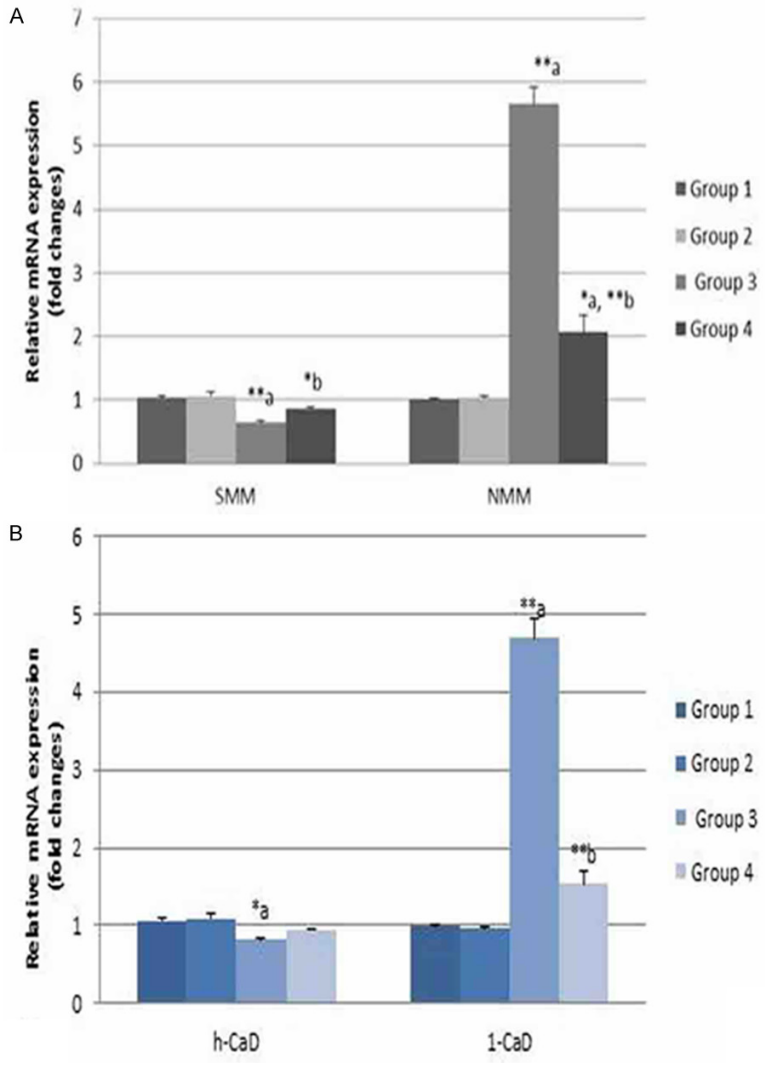

Figure 4. Real-time RT-PCR analysis in rat urinary bladder of the study groups. A: Expression of smooth muscle myosin (SMM) and non-muscle myosin (NMM). B: Expression of caldesmon isoforms; h-CaD and l-CaD. Expressions are normalized to GAPDH, the housekeeping gene. Values are expressed as mean ± standard error of means (SEM) of n = 6 animals; a: *P* value compared with group 1; b: *P* value compared with group 3; *: significant difference (P<0.05); **: highly significant difference (P<0.001).

Real-time PCR results

The real time RT-PCR analysis demonstrated no difference between group 1 and 2. Group 3 showed significant down regulation of SMM (0.64 fold) and h-CaD (0.81 fold) genes and up regulation of NMM (5.65 fold) and 1-CaD (4.7 fold) genes. Group 4 revealed non-significant changes in SMM, h-CaD and 1-CaD expression, while the NMM expression was significantly increased (2.07 fold) compared to group 1 (**Figure 4**).

Biochemical results for tissue antioxidant enzymes

Assay of CAT and SOD activities and NO levels were illustrated in (**Table 1**) after statistical analysis.

Morphometric results

Our statistically analyzed results for epithelial and muscle thickness measurements were represented in (**Table 2**). The number of anti-Ki-67 immunostained cells, the area percentage of positive anti-muscle actin immunoreactivity and the number of mast cells were summarized in (**Table 3**).

Discussion

showed positive nuclear reaction in few urothelial cells (**Figure 3A**). Group 3 revealed many positive urothelial cells (**Figure 3B**). In Group 4, few positive cells were seen (**Figure 3C**).

Examination of the sections stained for muscle actin revealed positive cytoplasmic reactions of myocytes in group 1 (**Figure 3D**). Group 3 showed increased positive immunoreactions compared with control (**Figure 3E**). The immunoreactions in group 4 were near normal (**Figure 3F**).

Prevalence and seriousness of lower urinary tract symptoms increase with age [32]. Numerous complications can happen in cases of partial urinary bladder obstruction [33].

In the current study, obstructed rats showed increase in epithelial thickness which was confirmed by morphometric analysis. This might be explained by the epithelial hyperplasia. The enhanced proliferation of the epithelium was evident by the highly significant increase in number of positive immunoreactions for the

Table 1. Catalase (CAT), superoxide dismutase (SOD) and nitric oxide (NO) levels in different groups

	Group 1	Group 2	Group 3	Group 4
CAT (U/mg protein)	15.67 ± 0.76	16.50 ± 0.76	7.33 ± 0.67**,a	13.67 ± 0.56**,b
SOD (U/mg protein)	0.52 ± 0.014	0.49 ± 0.011	0.26 ± 0.014**,a	0.47 ± 0.013*,a,**,b
NO	132.83 ± 2.43	124.83 ± 2.57	211.83 ± 3.28**,a	141.17 ± 3.71**,b

Values are expressed as mean ± standard error of means (SEM) of n = 6 animals; a: *P* value compared with group 1; b: *P* value compared with group 3; *: significant difference (P<0.05); **: highly significant difference (P<0.001).

Table 2. Epithelial and muscle thickness of different groups

	Group 1	Group 2	Group 3	Group 4
Epithelial thickness (μm)	41.12 ± 1.36	40.83 ± 1.61	68.79 ± 2.07**,a	45.60 ± 1.71**,b
Muscle thickness (mm)	0.82 ± 0.024	0.86 ± 0.029	1.57 ± 0.036**,a	0.91 ± 0.036**,b

Values are expressed as mean ± standard error of means (SEM) of n = 6 animals; a: *P* value compared with group 1; b: *P* value compared with group 3; **: highly significant difference (P<0.001).

Table 3. Number of anti-Ki-67 immune-stained cells, area percentage of positive anti-muscle Actin immune reactivity and the number of mast cells in different groups

	Group 1	Group 2	Group 3	Group 4
Anti-Ki-67	3.83 ± 0.6	4.17 ± 0.6	17.67 ± 1.28**,a	5.67 ± 0.76**,b
Anti-muscle Actin	48.33 ± 2.78	46.67 ± 2.4	83.33 ± 2.31**,a	60.83 ± 5.47*,b
Mast cells	0.33 ± 0.21	0.17 ± 0.17	4.50 ± 0.43**,a	0.83 ± 0.43**,b

Values are expressed as mean ± standard error of means (SEM) of n = 6 animals; a: *P* value compared with group 1; b: *P* value compared with group 3; *: significant difference (P<0.05); **: highly significant difference (P<0.001).

cell proliferation marker, Ki-67, compared with the control. Transitional epithelium exhibits a great ability to turnover within 24-48 h, in response to injury [34]. The mechanical stretch stress could increase the expression of several mitogens acting on urothelial cells [35], such as epidermal growth factor (EGF) [36], transforming growth factor-alpha and fibroblast growth factor [37].

In contrast, we observed some epithelial cells with apoptotic nuclei and inflammatory cell infiltrations in obstructed rats. Inflammation increases major cytokines such as tumor necrosis factor (TNF-α), interleukin (IL-6) and inducible nitric oxide synthase (iNOS) which in turn stimulate apoptosis [38].

Our ultrastructure examination of the epithelial cells revealed wide separations between cells which could be explained by disruption of urothelial junctional complexes. Our findings were in consensus with other researchers [39] who speculated that altered E-cadherin and a-catenin expression may be involved in disintegration of the cell-cell adhesion. We also recorded vacuolations of the cytoplasm of epithelial cells which could be explained by increased permeability of the urothelium due to obstruction [40].

In the present work, obstructed rats showed a highly significant increase in the muscle layer thickness compared with the control. This could be explained by hypertrophy of the muscle fibers. We recorded a strong expression of muscle actin immune-reactivity. Real-time RT-PCR analysis revealed significant down regulation of smooth muscle myosin (SMM) and h-CaD mRNA and up regulation of non-muscle myosin NMM and 1-CaD mRNA. Our results were in agreement with other authors who illustrated that PBOO altered detrusor SMM isoforms composition with overexpression of NMM. They also added that the contractility of detrusor muscle was attenuated and switched from phasic to more tonic [41, 42]. Mechanical stretch stresses change gene expression and transcription in epithelial cells and smooth muscle cells that deregulate the synthesis of many proteins and enzymes, including contractile cytoskeleton proteins and proteins regulating extracellular matrix deposition [43]. In the same context, our ultra-structural results revealed widened spac-

es between muscle cells with enhanced deposition of collagen fibers. The aggregated collagen fibers result in stiffening of the bladder wall, which may be the main cause of voiding dysfunction [44].

Our morphometric results revealed a highly significant increase in the number of mast cells in the bladder tissues of obstructed rats compared with the control. It was postulated that destroyed or dysfunctional urothelial cells produce cytokines such as stem cell factor that can stimulate proliferation and activation of mast cells [45]. The increased number of mast cells containing 5-hydroxytryptamine (5-HT) induces bladder contraction, that may be related to the storage symptoms in patients with BOO [46].

Oxidative stress is postulated to take a role in bladder pathology. Nitric oxide cooperates with the superoxide radical to generate peroxynitrite, one of the most toxic reactive nitrogen species [47]. In the current study, oxidative stress was evaluated. There were highly significant decreases in catalase (CAT) and superoxide dismutase (SOD) activities and a highly significant increase in nitric oxide (NO) level compared with the control. Similar results were reported by other researchers [48].

The alleviative effects of antioxidants on bladder dysfunction in animal models of PBOO gave the evidence for the role of oxidative injury in obstructed bladder [49, 50]. Kaempferol, a flavonoid present in various natural plants, is a potent peroxynitrite scavenger [51]. Upon co-administration of kaempferol, we revealed an improvement of the structural and ultrastructural changes of bladder induced by PBOO.

We recorded a highly significant decrease in Ki-67 and muscle actin immunohistochemical expressions compared with the obstructed group. Real-time RT-PCR analysis showed up regulation of SMM and h-CaD mRNA and down regulation of NMM and 1-CaD mRNA compared with the obstructed group. The anti-proliferative effect of Kaempferol could be attributed to its capability to induce nuclear DNA degradation and cell cycle arrest [52]. Kaempferol inhibits the activity of several enzymes involved in cell growth and signal transduction pathway [53].

Kaempferol attenuates tissue inflammation by its potent ability to inhibit expression of pro-inflammatory cytokines by inflammatory cells [54]. Regarding mast cells, our study showed highly significant decrease in their number compared with the obstructed group. This was explained by the anti-allergic and anti-asthmatic activities of kaempferol via inhibiting IgE mediated release of pro-inflammatory mediators [55].

In the current study, kaempferol effectively suppressed PBOO-induced oxidative stress. Kaempferol co-treatment provided significant increase in CAT and SOD activities and highly significant decrease in NO level compared to the obstructed group. In line with our observations, previous study reported that kaempferol inhibited protamine sulphate induced ROS formation in urinary bladder [56]. Kaempferol is considered an inhibitor of inducible nitric oxide synthase (iNOS) that inhibits NO production, and also it removes the cytotoxic effects of nitric oxide [20, 57].

In conclusion, PBOO induced deleterious histopathological changes, increase in Ki-67 and muscle Actin immune expressions, down regulation of SMM and h-CaD mRNA and up regulation of NMM and 1-CaD mRNA and enhancement of tissue oxidative stress markers. Kaempferol effectively reversed these alterations. The potency of kaempferol was correlated well with its antioxidant, anti-proliferative and anti-inflammatory capacity. The clinical application of kaempferol could represent a novel approach for counteracting bladder injury due to PBOO. Further, it is recommended to consume foods enriched in kaempferol especially in old age.

Disclosure of conflict of interest

None.

Address correspondence to: Asmaa AA Kattaia, Department of Histology and Cell Biology, Faculty of Medicine, Zagazig University, Zagazig, Asharquia 44519, Egypt. Tel: +201220723273; E-mail: asmaa-alhosiny7@gmail.com; ehabmohomar@yahoo.com

References

[1] Park JS, Lee CY, Lee W, Lee JZ. The effect of terazosin on the histological changes of rat

bladder after partial outlet obstruction. J Korean Continence Soc 2006; 10: 106-15.
[2] Dmochowski RR. Bladder outlet obstruction: etiology and evaluation. Rev urol 2005; 7 Suppl 6: S3.
[3] Andersson KE, Arner A. Urinary bladder contraction and relaxation: physiology and pathophysiology. Physiol Rev 2004; 84: 935-986.
[4] Oelke M, Kirschner, Hermanns R, Thiruchelvam N, Heesakkers J. Can we identify men who will have complications from benign prostatic obstruction (BPO)?: ICI-RS 2011. Neurourol Urodyn 2012; 31: 322-6.
[5] Nitti VW. Primary bladder neck obstruction in men and women. Rev Urol 2005; 7 Suppl 8, S12.
[6] Hypolite JA, DiSanto ME, Zheng Y, Chang S, Wein AJ, Chacko S. Regional variation in myosin isoforms and phosphorylation at the resting tone in urinary bladder smooth muscle. Am J Physiol Cell Physiol 2001; 280: C254-C264.
[7] Rhee AY, Ogut O, Brozovich FV. Nonmuscle myosin, force maintenance, and the tonic contractile phenotype in smooth muscle. Pflügers Arch 2006; 452: 766-774.
[8] Marston SB, Redwood CS. The molecular anatomy of caldesmon. Biochem J 1991; 279: 1.
[9] Yang L, Wang S, Cheng HP. Effect of long-term partial bladder outlet obstruction on caldesmon isoforms and their correlation with contractile function. Acta Pharmacol Sin 2008; 29: 600-605.
[10] M Calderon-Montano J, Burgos-Morón E, Pérez-Guerrero C, López-Lázaro M. A review on the dietary flavonoid kaempferol. Mini Rev Med Chem 2011; 11: 298-344.
[11] Weseler AR, Ruijters EJ, Drittij-Reijnders MJ, Reesink KD, Haenen GR, Bast A. Pleiotropic benefit of monomeric and oligomeric flavanols on vascular health-a randomized controlled clinical pilot study. PLoS One 2011; 6: e28460.
[12] Choi EM. Kaempferol protects MC3T3-E1 cells through antioxidant effect and regulation of mitochondrial function. Food Chem Toxicol 2011; 49: 1800-1805.
[13] Wang L, Tu YC, Lian TW, Hung JT, Yen JH, Wu MJ. Distinctive antioxidant and antiinflammatory effects of flavonols. J Agric Food Chem 2006; 54: 9798-804.
[14] Athar M, Back JH, Tang X, Kim KH, Kopelovich L, Bickers DR Kim AL. Resveratrol: a review of preclinical studies for human cancer prevention. Toxicol Appl Pharmacol 2007; 224: 274-283.
[15] Kris-Etherton PM, Keen CL. Evidence that the antioxidant flavonoids in tea and cocoa are beneficial for cardiovascular health. Curr Opin lipidol 2002; 13: 41-49.
[16] Wattel A, Kamel S, Mentaverri R, Lorget F, Prouillet C, Petit JP, Brazier M. Potent inhibitory effect of naturally occurring flavonoids quercetin and kaempferol on in vitro osteoclastic bone resorption. Biochem Pharmacol 2003; 65: 35-42.
[17] Serretta V, Morgia G, Fondacaro L, Curto G, Pirritano D, Melloni D, Orestano F, Motta M, Pavone-Macaluso M; Members of the Sicilian-Calabrian Society of Urology. Open prostatectomy for benign prostatic enlargement in southern Europe in the late 1990s: a contemporary series of 1800 interventions. Urology 2002; 60: 623-7.
[18] Bigoniya P, Singh CS, Shrivastava B. In vivo and in vitro hepatoprotective potential of kaempferol, a flavone glycoside from Capparis spinosa. IJPBS 2013; 3: 139-52.
[19] de Sousa E, Zanatta L, Seifriz I, Creczynski-Pasa TB, Pizzolatti MG, Szpoganicz B, Silva FR. Hypoglycemic Effect and Antioxidant Potential of Kaempferol-3, 7-O-(α)-dirhamnoside from Bauhinia f orficata Leaves. J Nat Prod 2004; 67: 829-832.
[20] Mahat MY, Kulkarni NM, Vishwakarma SL, Khan FR, Thippeswamy BS, Hebballi V, Adhyapak AA, Benade VS, Ashfaque SM, Tubachi S, Patil BM. Modulation of the cyclooxygenase pathway via inhibition of nitric oxide production contributes to the anti-inflammatory activity of kaempferol. Eur J Pharmacol 2010; 642: 169-76.
[21] Goi Y, Tomiyama Y, Yokoyama A, Tatemichi S, Maruyama K, Kobayashi M, Yamaguchi O. Effect of silodosin, a selective α 1A-adrenoceptor antagonist, on voiding behavior and bladder blood flow in a rat model of bladder outlet obstruction. Eur J pharmacol 2015; 764: 489-96.
[22] Liu F, Yao L, Yuan J, Liu H, Yang X, Qin W, Wu G, Yang L, Wang H, Takahashi N, Yamaguchi O. Protective effects of inosine on urinary bladder function in rats with partial bladder outlet obstruction. Urology 2009; 73: 1417-22.
[23] Kim JC, Yoo JS, Park EY, Hong SH, Seo SI, Hwang TK. Muscarinic and purinergic receptor expression in the urothelium of rats with detrusor overactivity induced by bladder outlet obstruction. BJU Int 2008; 101: 371-375.
[24] Sakai T, Kasahara K, Tomita K, Ikegaki I, Kuriyama H. 5-Hydroxytryptamine-induced bladder hyperactivity via the 5-HT2A receptor in partial bladder outlet obstruction in rats. Am J Physiol Renal Physiol 2013; 304: F1020-1027.
[25] Bancroft JD, Gamble M. Connective tissue stains. In: Bancroft JD, Gamble M, editors. Theory and practice of histological techniques. 6th edition. London, New York, Philadelphia: Churchill Livingstone; 2007. pp. 150.
[26] Ayache J, Beaunier L, Boumendil J, Ehret G, Laub D. Sample preparation handbook for transmission electron microscopy: techniques.

New York USA: Springer Science & Business Media; 2010.
[27] Ramos-Vara JA, Kiupel M, Baszler T, Bliven L, Brodersen B, Chelack B, Czub S, Del Piero F, Dial S, Ehrhart EJ, Graham T, Manning L, Paulsen D, Valli VE, West K; American Association of Veterinary Laboratory Diagnosticians Subcommittee on Standardization of Immunohistochemistry. American association of veterinary laboratory diagnosticians' subcommittee on standardization of immunohistochemistry suggested guidelines for immunohistochemical techniques in veterinary diagnostic laboratories. J Vet Diagn Invest 2008; 20: 393-413.
[28] Aebi H. Catalase. In: Methods of Enzymatic Analysis. Bergmeyer HU (Edition). New York, NY, USA: Academic Press; 1974. pp. 673-677.
[29] Sun Y, Oberley LW, Li YA. Simple method for clinical assay of superoxide dismutase. Clin Chem 1988; 34: 497-500.
[30] Misko TP, Schilling RJ, Salvemini D, Moore WM, Currie MG. A fluorometric assay for the measurement of nitrite in biological samples. Anal Biochem 1993; 214: 11-16.
[31] Petrie A, Sabin C. Basic techniques for analysing data. In Medical statistics at a glance. 2nd edition. In: Sugden M, Moore K editors. USA: Blackwell Publishing Ltd; 2005. pp. 55-56.
[32] Bailey K, Abrams P, Blair PS, Chapple C, Glazener C, Horwood J, Lane JA, McGrath J, Noble S, Pickard R, Taylor G, Young GJ, Drake MJ, Lewis AL. Urodynamics for Prostate Surgery Trial; Randomised Evaluation of Assessment Methods (UPSTREAM) for diagnosis and management of bladder outlet obstruction in men: study protocol for a randomised controlled trial. Trials 2015; 16: 567.
[33] Aitken KJ, Bägli DJ. The bladder extracellular matrix. Part I: architecture, development and disease. Nat Rev Urol 2009; 6: 596-611.
[34] Lendvay TS, Sweet R, Han CH, Soygur T, Cheng JF, Plaire JC, Charleston JS, Charleston LB, Bagai S, Cochrane K, Rubio E, Bassuk JA. Compensatory paracrine mechanisms that define the urothelial response to injury in partial bladder outlet obstruction. Am J Physiol Renal Physiol 2007; 293: F1147-F1156.
[35] Chaqour B, Whitbeck C, Han JS, Macarak E, Horan P, Chichester P, Levin R. Cyr61 and CTGF are molecular markers of bladder wall remodeling after outlet obstruction. Am J Physiol Endocrinol Metab 2002; 283: E765-E774.
[36] Southgate J, Hutton KA, Thomas DF, Trejdosiewicz LK. Normal human urothelial cells in vitro: proliferation and induction of stratification. Lab Invest 1994; 71: 583-94.
[37] De Boer WI, Vermeij M, Diez DM, Bindels E, Radvanyi F, Van der Kwast T, Chopin D. Functions of fibroblast and transforming growth factors in primary organoid-like cultures of normal human urothelium. Lab Invest 1996; 75: 147-156.
[38] Bonvissuto G, Minutoli L, Morgia G, Bitto A, Polito F, Irrera N, Altavilla D. Effect of Serenoarepens, lycopene, and selenium on proinflammatory phenotype activation: an in vitro and in vivo comparison study. Urology 2011; 77: 248-e9.
[39] Celik-Ozenci C, Ustunel I, Erdogru T, Seval Y, Korgun ET, Baykara M, Demir R. Ultrastructural and immunohistochemical analysis of rat uroepithelial cell junctions after partial bladder outlet obstruction and selective COX-2 inhibitor treatment. Acta Histochemica 2006; 107: 443-451.
[40] Araki I, Du S, Kamiyama M, Mikami Y, Matsushita K, Komuro M, Takeda M. Overexpression of epithelial sodium channels in epithelium of human urinary bladder with outlet obstruction. Urology 2004; 64: 1255-1260.
[41] Zhang EY, Stein R, Chang S, Zheng Y, Zderic SA, Wein AJ, Chacko S. Smooth muscle hypertrophy following partial bladder outlet obstruction is associated with overexpression of nonmuscle caldesmon. Am J Pathol 2004; 164: 601-12.
[42] Zhang X, Seftel A, DiSanto ME. Blebbistain, a myosin II inhibitor, as a novel strategy to regulate detrusor contractility in a rat model of partial bladder outlet obstruction. PLoS One 2011; 6: e25958.
[43] Mirone V, Imbimbo C, Longo N, Fusco F. The detrusor muscle: an innocent victim of bladder outlet obstruction. Eur Urol 2007; 51: 57-66.
[44] Yang X, Li YZ, Mao Z, Gu P, Shang M. Effects of estrogen and tibolone on bladder histology and estrogen receptors in rats. Chin Med J 2009; 122: 381-5.
[45] Theoharides TC, Kempuraj D, Sant GR. Mast cell involvement in interstitial cystitis: a review of human and experimental evidence. Urology 2001; 57 Suppl 1: 47-55.
[46] Michishita M, Tomita KI, Yano K, Kasahara KI. Mast Cell Accumulation and Degranulation in Rat Bladder with Partial Outlet Obstruction. Adv Ther 2015; 32: 16-28.
[47] Birder LA, Wolf-Johnston A, Buffington CA, Roppolo JR, De Groat WC, Kanai AJ. Altered inducible nitric oxide synthase expression and nitric oxide production in the bladder of cats with feline interstitial cystitis. J Urol 2005; 173: 625-629.
[48] Callaghan CM, Schuler C, Leggett RE, Levin RM. Effect of severity and duration of bladder outlet obstruction on catalase and superoxide dismutase activity. Int J Urol 2013; 20: 1130-1135.

[49] Conners W, Whitebeck C, Chicester P, Legget R, Johnson A, Kogan B, Conners W, Whitebeck C, Chicester P, Legget R, Lin AD, Johnson A, Kogan B, Levin R, Mannikarottu A. L-NAME, a nitric oxide synthase inhibitor, diminishes oxidative damage in urinary bladder partial outlet obstruction. Am J Physiol Renal Physiol 2006; 290: F357-363.

[50] Hong SK, Son H, Kim SW, Oh SJ, Choi H. Effect of glycine on recovery of bladder smooth muscle contractility after acute urinary retention in rats. BJU Int 2005; 96: 1403-1408.

[51] Heijnen CG, Haenen GR, Van Acker FA, Van der Vijgh WJ, Bast A. Flavonoids as peroxynitrite scavengers: the role of the hydroxyl groups. Toxicology in vitro 2001; 15: 3-6.

[52] Kuntz S, Wenzel U, Daniel H. Comparative analysis of the effects of flavonoids on proliferation, cytotoxicity, and apoptosis in human colon cancer cell lines. Eur J nut 1999; 38: 133-142.

[53] Landolfi R, Mower RL, Steiner M. Modification of platelet function and arachidonic acid metabolism by bioflavonoids: structure-activity relations. Biochem Pharmacol 1984; 33: 1525-1530.

[54] Devi KP, Malar DS, Nabavi SF, Sureda A, Xiao J, Nabavi SM, Daglia M. Kaempferol and inflammation: From chemistry to medicine. Pharmcol Res 2015; 99: 1-10.

[55] Kempuraj D, Madhappan B, Christodoulou S, Boucher W, Cao J, Papadopoulou N, Cetrulo CL, Theoharides TC. Flavonols inhibit proinflammatory mediator release, intracellular calcium ion levels and protein kinase C theta phosphorylation in human mast cells. Br J Pharmacol 2005; 145: 934-944.

[56] Huang YB, Lin MW, Chao Y, Huang CT, Tsai YH, Wu PC. Anti-oxidant activity and attenuation of bladder hyperactivity by the flavonoid compound kaempferol. Int J Urol 2014; 21: 94-98.

[57] Hämäläinen M, Nieminen R, Vuorela P, Heinonen M, Moilanen E. Anti-inflammatory effects of flavonoids: genistein, kaempferol, quercetin, and daidzein inhibit STAT-1 and NF-κB activations, whereas flavone, isorhamnetin, naringenin, and pelargonidin inhibit only NF-κB activation along with their inhibitory effect on iNOS expression and NO production in activated macrophages. Mediat Inflamm 2007; 2007: 45673.